periodica polytechnica

Transportation Engineering
39/2 (2011) 49–54
doi: 10.3311/pp.tr.2011-2.01
web: http://www.pp.bme.hu/tr

RESEARCH ARTICLE

Preliminary results of active centrifugal compressor surge control using variable inducer shroud bleed

Károly Beneda

Received 2010-09-06

Abstract

The goal of this paper is to give a short introduction to the reader into the preliminary results of the practical investigations of active centrifugal compressor surge control using variable inducer shroud bleed (VISB). After establishing the mathematical model of the VISB researches are being carried out on a compressor. There is a detailed description of the measurement equipment which covers a test bench and a data acquisition system. With the measurement and evaluation of the thermodynamic operational parameters of the compressor system, the theoretical investigation can be validated, which is also presented hereby.

Keywords

Centrifugal compressor · variable inducer shroud bleed · surge control

Károly Beneda

Department of Aircraft and Ships, BME, Stoczek u. 6. H-1111 Budapest, Hungary

e-mail: beneda@rht.bme.hu

1 Introduction

An electrically driven compressor testbench is under development for evaluation of dynamic mathematical models of active surge control devices at the Department of Aircraft and Ships of BUTE. This equipment includes a centrifugal compressor which is a commonly used device in aircraft for propulsion and auxiliary power source and is also wide-spread in the industry [6]. Therefore the investigation and possibilities for suppressing the compressor instabilities has been important for decades and becomes even more emphasized nowadays. The centrifugal compressor surge suppression counts numerous methods that are available in current products and there are also some possibilities for development [2]. The inducer shroud bleed as a passive, fixed geometry solution has been widely spread but unfortunately has disadvantages at higher mass flow rates. The idea of modulating outflow cross section is to obtain surge avoidance capabilities at low flow with opened orifices and closing them at higher mass flow leads to improving efficiency. In this paper the measurement system and the preliminary results of the experimental investigation are detailed.

2 The electrically driven compressor test bench

The Department of Aircraft and Ships has an electrically driven centrifugal compressor that is another possible equipment for surge control researches. This test rig incorporates a three phase variable frequency drive for controlling the electric motor speed. Thus through an accelerating gearbox transmission the compressor speed can be varied and maintained at the desired value easily.

2.1 The compressor

The focus of the investigation is on a GANZ type industrial centrifugal compressor (see Fig. 1). The impeller of the compressor has 16 radial blades with integrated inducer. Its operating speed range covers 5..20 krpm which is realized using a three phase frequency controlled asynchronous AC motor with an accelerating gearbox.

The GANZ compressor has a small radial vaned diffuser and a volute that collects the compressed air. In the scroll outlet there

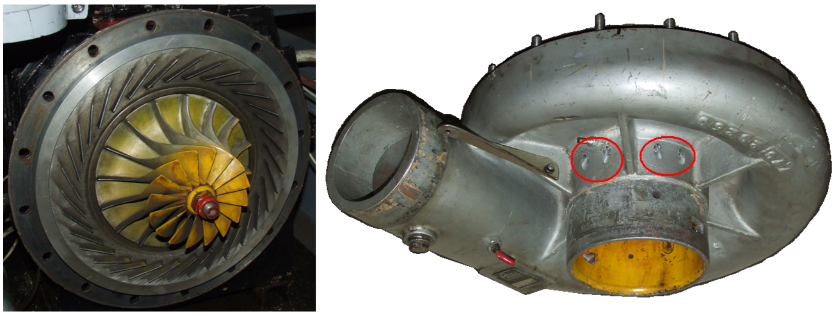

Fig. 1. The impeller of the GANZ compressor with scroll removed (left) and the modified scroll with shroud bleed orifices (right)

is a butterfly throttle valve which has been previously installed for controling purposes. Close coupled resistances (throttle orifices) has been thouroughly investigated in the mid 1970's ([4]) and results have shown that such devices can cause a shift of the compressor characteristic to the lower mass flow rates. Taking into account this effect the throttle valve itself will also affect the surge behaviour of the system. The common implementation of a compression system is shown on Fig. 2 [8].

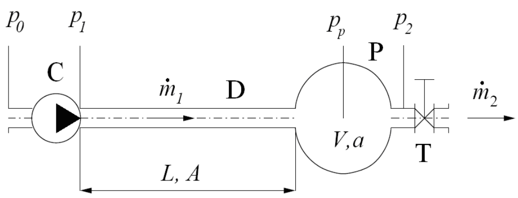

Fig. 2. The schematic of the compression system [8]

The GANZ compressor installed at the laboratory of the Department originally delivers compressed air for an air cycle machine and a heat exchanger unit for demonstration of environmental control systems for educational purposes. Therefore a long ducting can be found of diameter $D = 0.125m$ and length $L = 3.4m$ connecting the source and the destination. Around the heat exchanger there is a collecting plenum that has a volume of $V_P = 0.04m^3$. Regarding to Greitzer's work [9] these parameters can be combined to give a description of the system behavior as shown in Eq. 1 which is called dimensionless stability parameter or behavior B and its value for the given equipment is approximately $B \approx 0,25$.

$$B = \frac{u}{2\omega_H L_C} = \frac{u}{2a_P}\sqrt{\frac{V_P}{A_C L_C}} \approx 0,25 \qquad (1)$$

Researches have shown that the dimensionless flow factor ϕ has a threshold over which uniform flow pattern can be established, under which the instabilities can take place. Depending on the flow factor ϕ and stability parameter B various forms of instabilities can emerge. It has been proven both experimentally and theoretically ([3]) that the increasing B leads to more and more severe instabilities. It can be visualized through the diagram shown in Fig. 3.

It can be seen from Eq. 1 that for a given equipment the Greitzer behavior parameter depends linearly on the blade tip speed

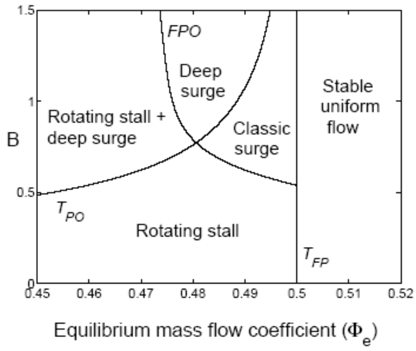

Fig. 3. Instability phenomena as a function of flow factor ϕ and stability parameter B from [8]

u which can explain why surge occurs in the high speed region of operation. If one compares Fig. 3 and the result of Eq. 1 for the given compressor, it is obvious that without modification of the system (plenum volume, ducting, etc.) the only possible instability form is rotating stall.

2.2 The data acquisition system

The data acquisition for the GANZ compressor test rig uses the experiences gathered formerly creating the measurement system for other gas turbines at the Department. It is based also on the LabVIEW™ up-to-date graphical programming environment that communicates through an RS-232 serial channel with a HBM Spider8 standalone data acquisition device. The Spider8 allows simultaneous measurements on eight channels with a resolution of 16 bits. Although its sample rate can reach 9600 samples/sec/channel, in the current configuration (mainly constrained by the serial communication) is about 10 samples/sec/channel [7]. The following pressure values are monitored by the system:

- ambient pressure (MPX4115A) 15-115kPa absolute
- compressor inlet (MPX5010DP) 10kPa gauge
- inlet orifice (MPX5010DP) 10kPa gauge
- compressor surge control plane (MPXV7007DP) ±7kPa gauge or vacuum
- compressor outlet total pressure (MPX5050DP) 0-50kPa gauge

The software also gathers temperature data from a J type (iron-constantan) thermocouple which is installed at the compressor outlet and a rotary potentiometer that gives feedback signal of the close coupled downstream throttle valve. The rotational speed of the compressor is recorded only manually because the variable speed electric drive has a frequency display which shows current values with a resolution of 1/10th Hertz that means the compressor speed can be determined with an accuracy of ± 6 rpm. Therefore the optical measuring device, which is under development, is not urgent to introduce as the measurements are carried out at predetermined constant speeds that do not change during the measurements due to the electric drive.

The throttle valve has a microcontroller board that is responsible for driving a DC servo motor. The microcontroller unit (MCU) is a Freescale MC9S08QD4 IC with 8-bit architecture main features of which are the integral 10-bit A/D converter, interrupt module and pulse width modulation (PWM) output. Their function is as follows:

- The A/D converter is necessary to create any arbitrary output on the PWM module to position the servo if manual control is needed.
- The interrupt module is responsible for starting the throttling cycle if a trigger (falling) edge is detected. This is realized now with a manual pushbutton, that will be superseded by a digital output of the Spider8 hardware.
- The PWM module creates the standard servo drive signal, which is an asymmetric square with a period of $T = 20ms$ and a variable pulse width from a minimum of $t_{P,min} = 1ms$ up to a maximum of $t_{P,max} = 2ms$. In this application, neither limit can be reached due to mechanical constraints.

The program contains an algorithm to make the motor travel slowly (with around 1 degree/s angular speed) from one stop to the other thus moving the throttle valve from fully open to the minimally open position. This way a timed movement of the valve can be produced eliminating the uncertainties when only manual driving would be present. This plays a main role in accurately determining the surge precedence and onset parameters. The servo equipment is shown on Fig. 4.

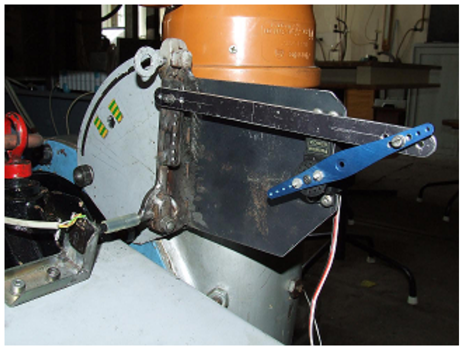

Fig. 4. The DC servo motor drive of the throttle valve downstream of the compressor

2.3 The measurements

The measurements carried out until now include the recording of compressor characteristics at predetermined constant speeds in two separate section using the close coupled throttling and no inducer shroud bleed used as the devices are under construction yet:

1. the first group of measurements ranging from 40 up to 100 percent of nominal speed with 10 percent steps. This was used for detailed investigation of the characteristic at the selected speeds with mass flow rates far below the instability limit. The minimum open position of the throttle valve was actually the fully closed one;
2. the range of the second group covered the 40 up to 110 percent nominal speed with 5 percent steps. This was an accelerated test compared to the previous, included a narrower mass flow range reaching just below the surge limit. The throttle valve was not driven therefore fully closed during this test.

Both measurements have been carried out using the MCU based throttle control. Each constant speed recording included five travels of the throttle valve from the open to the minimal open position and back. The small speed of the DC servo motor caused the opening cycle to be at around 50 seconds. Considering its half, 25 seconds for a throttling is a quite slow change therefore it can be taken into account as quasi-steady state measurement. The five repetitions are necessary for accuracy to produce enough number of recorded operational parameters.

The GANZ compressor is equipped now with the measurement capability of the wall static pressure at the planned cross section of the VISB. This allows a preliminary comparison between the recorded data using no shroud bleed and the calculated surge control effect based on measured wall static pressures that would be the driving force of bleeding a specified mass flow out of the inducer outlet.

3 The mathematical model

3.1 The Split Compression Model (SCM)

The centrifugal compressor inducer shroud bleed (either fixed or variable) can be investigated with the help of the Split Compression Model (SCM) developed by the author formerly [1]. This method treats the centrifugal compressor as a combination of two elements in series: the inducer and the impeller passages. At the connecting surface there is the variable shroud bleed implemented which divides the inducer mass flow in two parts, the one that enters the impeller and thus the user system, and the one that is bled through the orifices into the atmosphere (as it is under development on the GANZ compressor) or a closed chamber.

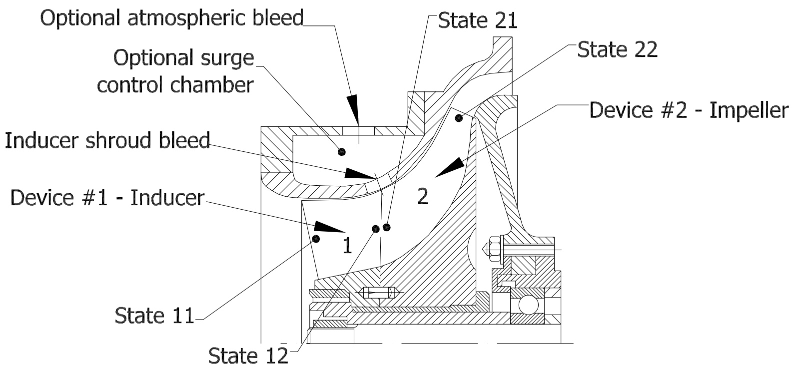

Fig. 5. The schematic of compressor division for mathematical modeling

The mathematical model treats the variable inducer shroud bleed as simple orifices which have a normalized opening of γ_{SB} that is simply the ratio of the actual and maximal area of the orifices defined as

$$\gamma_{SB} = \frac{A_{SB\mathrm{act}}}{A_{SB\max}} \tag{2}$$

This means the normalized shroud bleed opening range is 0..1. The model then calculates the inducer pressure ratio which in turn will cause a bleed air flow returning to the atmosphere or entering the control chamber. Under certain circumstances (i.e. mass flow rate is too high or too low) the wall static pressure at the surge control plane decreases below ambient resulting in a suction effect causing the impeller mass flow to increase.

3.2 Governing equations

The SCM computation is based on a one-dimensional analysis using enthalpy relationship between work input and pressure rise inside the inducer and impeller. The model uses the following data as input: the rotational speed n, which is equal for inducer and impeller, the ambient temperature T_0 and pressure p_0, and outlet mass flow $\dot{m}$, which depends on the throttling characteristics of the user system. It is to be emphasized that outlet mass flow is needed as the inlet mass flow is a result of the calculations.

The change in stagnation enthalpy Δh_i^* (where * denotes the parameter is stagnational) is equal to the change of the product of tangential velocities (c_{iu}) and blade speeds (u_i) at the outlet and the inlet of the i^{th} unit can be determined using Eq. 3. Blade speeds are to be determined by the rotational speed and device geometry.

$$\Delta h_i^* = u_{i2} p c_{i2u} - u_{i1} p c_{i1u} \tag{3}$$

The inlet tangential velocities are considered as predetermined values. The c_{11u} is given by the inlet prewhirl, while c_{21u} is equal to c_{12u} (see Fig. 5). Outlet tangential velocities can be estimated from the velocity triangle using slip factor μ. The slip factor of the inducer is considered to be equal to one.

$$c_{i2u} = \mu_i p u_{i2} \tag{4}$$

The change in stagnation enthalpy Δh_i^* can also be described as the change in stagnation temperature ΔT_i^* multiplied by the specific heat at constant pressure c_p.

$$\Delta h_i^* = c_p p \Delta T_i^* \tag{5}$$

The relations between stagnation temperatures and ideal pressures are to be determined from the Poisson equation for isentropic process:

$$\frac{p_{i2}^*}{p_{i1}^*} = \left(\frac{T_{i2}^*}{T_{i1}^*}\right)^{\frac{\kappa}{\kappa-1}} \tag{6}$$

After calculation of ideal pressures one can ascertain real pressure values taking various losses into account. The SCM is computing friction and curvature losses as standard pipe correlations using hydraulic diameter d_{hyd} and channel length l_{fric} based on Equations 7 and 8. Inlet shock losses are also considered as a function of deviation of inlet angle β from the nominal value β_{nom} as shown in Eq. 9. Shock losses occur only at the inducer inlet. The friction loss determination takes into account the fact that three faces of the channel (the impeller vane and hub) are in contact with the relative velocity w and the shroud is the only one for which the absolute velocity c is to be used. These are in Eq. 7 as Δp_w and Δp_c. As noted in [5], the friction coefficient λ, hydraulic diameter d_{hyd}, absolute and relative velocities (c and w, respectively) and the density ρ can be taken as average value (distinguished with an overline) computed from inlet and outlet data without considerable inaccuracy.

$$\Delta p_{fric} = \frac{1}{4} p \Delta p_c + \frac{3}{4} p \Delta p_w = \frac{1}{4} p \overline{\lambda}_c p \frac{l_{fric}}{\overline{d}_{hyd}} p \overline{\rho} p \frac{\overline{c}^2}{2} + \frac{3}{4} p \overline{\lambda}_w p \frac{l_{fric}}{\overline{d}_{hyd}} p \overline{\rho} p \frac{\overline{w}^2}{2} \tag{7}$$

$$\Delta p_{curv} = \zeta p \overline{\rho} \frac{\overline{c}^2}{2} \tag{8}$$

$$\Delta p_{shock} = \cos^2(\beta - \beta_{nom}) \tag{9}$$

Being acquainted with the pressures at the main cross sections the mass flow of bled air through the VISB $\dot{m}_{SB}$ can be estimated using the standard orifice correlation with contraction co-

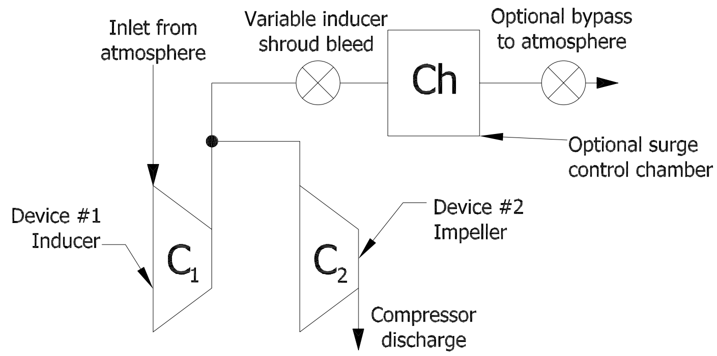

Fig. 6. The schematic of compressor division for mathematical modeling

efficient α_{SB}, density at VISB cross section ρ_{SB} and static pressure difference Δp_{SB} (Eq. 10).

$$\dot{m}_{SB} = \alpha_{SB} p \gamma_{SB} p A_{SBmax} p \sqrt{2 p \rho_{SB} p \Delta p_{SB}} \qquad (10)$$

4 Results

The mathematical model of the VISB is under validation using measurement data from the GANZ compressor. Although the mathematical model with the current configuration of measurement system has only been verified at the zero γ_{SB} value, some conclusions can be drawn based on general trends in wall static pressure variations at the shroud bleed orifice region as a function of the mass flow rate.

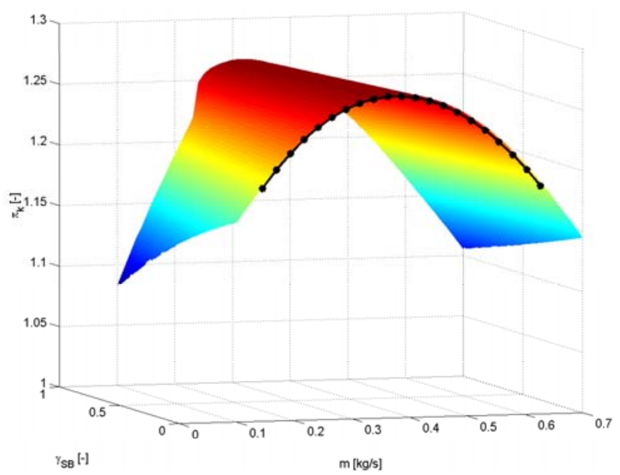

Fig. 7. Pressure ratio π_K as a function of $\dot{m}$ mass flow rate and γ_{SB} relative opening of shroud bleed orifices - surface: computed, black line: measured data

The results of the preliminary measurements for a selected rotational speed ($\overline{n} = 100\%$) are indicated in the mathematical model calculated compressor performance map shown in Fig. 7. The data acquired have been used to validate the model in the zero surge suppression domain and have given good matching between the theoretical computation and the experimental research. The whole surface needs some explanation as the measurements delivered until now only approximate relationship between the expected behaviour of the active surge suppression and the measured data, i.e. wall static pressures have only been evaluated and considered as a baseline for further investigations. On Fig. 7 there is a characteristic surface illustrated which has emerged from the traditional two-dimensional compressor characteristic curves taking into account another independent variable - the normalized shroud bleed - besides of the original mass flow rate. It can be seen on this surface that its sections at constant γ_{SB} form curves similar to the original (like the measured black line). The only difference is in the behaviour of the surface at very low mass flow rates combined with high γ_{SB} values. Under such circumstances the wall static pressure drops below ambient causing an inflow instead of outward bleed. It is interesting to take into account the effect of the increased impeller flow might suppress the onset of surge, even though the inducer operates in a stalled region.

The data acquired has been used for creating the nondimensional compressor characteristic map which is shown on Fig. 8. It is obvious that the stable uniform flow is only possible over the dimensionless flow coefficient $\phi = 0.15$ value.

5 Further developments

As it was emphasized throughout this paper only preliminary results of a diversified research are presented hereby. In the close future as the measurement system is almost at its final configuration the further developments will focus on creating the inducer bleed orifices as fixed holes on the compressor shroud (see Fig. 1). This modification itself will allow the measurement of the steady-state condition with maximum VISB opening.

The next step will be the design and implementation of a closing apparatus on the orifices thus gathering the ability to realize any normalized shroud bleed opening between 0 and 1. This can lead to the complete static modeling of the system and further analysis of behaviour in the time domain for establishing proper control laws of the surge control system operation.

References

1 **Beneda K**, *Dynamic Nonlinear Mathematical Model of Active Compressor Surge Control Devices*, 11th Mini Conference on Vehicle System Dynamics, Identification and Anomalies, 2008, pp. 583-591.

2 **Botros K K, Henderson J F**, *Developments in Centrifugal Compressor Surge Control*, Technology Assessment. ASME Journal of Turbomachinery **116** (April 1994), 240-249.

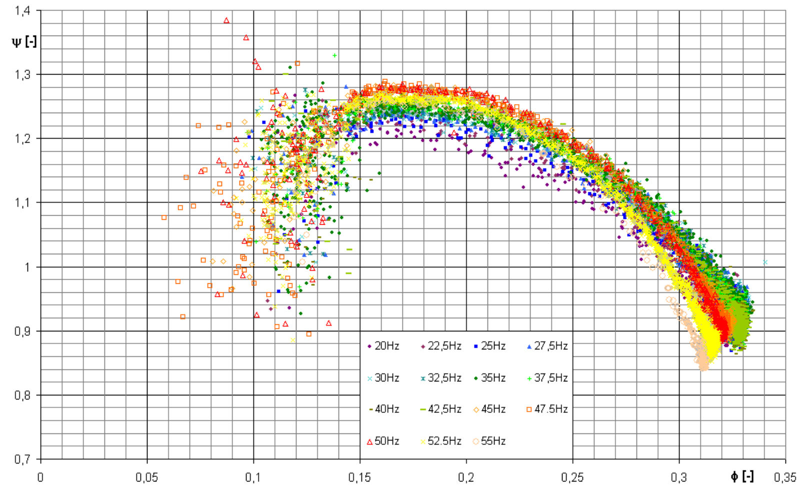

Fig. 8. Measured dimensionless flow factor ϕ versus dimensionless pressure rise ψ at various rotational speeds

3 **Cumpsty N A**, *Compressor Aerodynamics*, Longman, 1989.

4 **Dussourd J L, Pfannebecker G, Singhania S K**, *Consideration for the Control of Surge in Dynamic Compressors Using Close Coupled Resistances*, Centrifugal Compressor and Pump Stability, Stall and Surge, 1976.

5 **Ferguson T B**, *The Centifugal Compressor Stage*, Butterworths, London, 1963.

6 **Ffowcs Williams J E, Harper M F L, Allwright D J**, *Active Stabilization of Compressor Instability and Surge in a Working Engine*, ASME Journal of Turbomachinery **115** (January 1993), 68-75.

7 **Hottinger Baldwin Messtechnik GmbH**, *Spider8 Operating Manual*.

8 **Hős C, Kullmann L, Champneys A**, *Bifurcation Analysis of Surge and Rotating Stall in the Moore-Greitzer Compression System*, IMA Journal of Applied Mathematics **68** (April 2003), 205-228.

9 **Pampreen R C**, *Compressor surge and stall. Concepts ETI*, Norwich, 1993.